Confinement of CO_2 Inside (20,0) Single-Walled Carbon Nanotubes

Noelia Faginas-Lago[1(✉)], Andrea Lombardi[1], Yusuf Bramastya Apriliyanto[2], and Leonardo Pacifici[1]

[1] Dipartimento di Chimica, Biologia e Biotecnologie, Università degli Studi di Perugia, 06123 Perugia, Italy
noelia.faginaslago@unipg.it
[2] Department of Chemistry, Indonesia Defense University, Kampus Unhan Komplek IPSC Sentul, Bogor, Indonesia

Abstract. We present a preliminary report based on molecular dynamics (MD) simulations to study CO_2 adsorption on flexible single-walled carbon nanotubes (SWCNTs) of (20,0) size. The adsorption capacities of (20,0) SWCNT were simulated at different temperatures and the effects of its diameter and chirality were compared with a previous work of our group. The potential energy surfaces have been described by implementing the Improved Lennard Jones (ILJ) potential to specifically model the intermolecular interactions involving CO_2-CO_2 and CO_2-SWCNT pairs. The intramolecular interactions within the SWCNT were considered explicitly by employing the Morse and Harmonic potentials. These specialized potentials are well capable of defining CO_2 confinement through physisorption and guarantee a quantitative description and realistic results of molecular dynamics. Flexible (20,0) SWCNT can adsorb up to 32 wt% at 273 K, thus as sizable carbon structured materials, SWCNTs are potentially suitable for CO_2 confinement and storage to cope with CO_2 gas emission.

Keywords: SWCNT · Small gases molecules adsorption · Empirical potential energy surface · Improved Lennard-Jones

1 Introduction

Recent scientific reports have revealed that carbon dioxide emission to the atmosphere has significantly risen in the last decades [1]. Large-scale industrial activities such as manufacture materials processing (iron, steel, cement, etc.) and energy production (fossil fuel power plants), majorly contribute to this increasing trend [2]. This trend leads to many serious problems on earth, ranging from environmental pollution to a rising of global temperature along with its catastrophic climate change effects [3]. Therefore, it is urgent to implement strategies to turn the evolution trend, keeping the CO_2 at the current level or even reducing the CO_2 concentration in the atmosphere [4]. In order to achieve this goal,

© The Author(s), under exclusive license to Springer Nature Switzerland AG 2022
O. Gervasi et al. (Eds.): ICCSA 2022 Workshops, LNCS 13382, pp. 275–289, 2022.
https://doi.org/10.1007/978-3-031-10592-0_21

capturing CO_2 molecules in sites where they are generated or known as post-combustion carbon capture is widely accepted as the most efficient, effective and energetically feasible method [5]. However, the main constraint is that typically a post-combustion flue gas is in a form of mixture composed from water, carbon dioxide, oxygen and nitrogen molecules [6]. Various methods such as those involving liquid absorbents, solid adsorbents, and a hybrid of solid-liquid based materials have been reported to selectively capture CO_2 from flue gas [7–9]. Among those methods, carbon capture using solid adsorbents attracted global attention in the last few years [10,11]. This method offers major advantages, for instance for its simplicity and the relatively cheaper implementation on existing power plants [2,5]. Moreover, solid adsorbents have minimum chemical risks that usually arise with the use of traditional amine solvents (e.g. equipment corrosion, solvent evaporation, chemical stability, and unpleasant smells) [12].

The range of options of applicable solid adsorbents for carbon capture and separation is vast, only materials with high selectivity and high gravimetric uptake is the best suited option. Permeability also plays an important role, in which it corresponds to diffusion of gas inside the materials to produce effective gas adsorption [13]. In order to attain high gravimetric value, a material should have large surface area (adsorption sites) in combination with its lightweight structure. Large surface area is normally achieved by introducing intrinsic pores on a nanometer scale, thus obtaining so-called nanoporous materials. Moreover, intrinsic pores that are available inside the nanoporous materials also enhance the permeability of materials. A range of nanoporous materials for CO_2 capture and separation have been reported, for instance, zeolitic imidazolate frameworks (ZIFs) and zeolites [14,15], porous polymer networks (PPNs) or covalent organic polymers/frameworks (COPs/COFs) [16–18], metal-organic frameworks (MOFs) [19,20], and nanoporous carbons [21–23].

In particular, carbon-based materials exhibit desirable electronic and physicochemical properties (e.g. chemically inert, relatively high hydrophobicity and thermally stable). Moreover, they are composed from lightweight carbon atoms producing low density and stable structures [24,25]. In contrast, MOFs and zeolites-based materials despite showing good gas uptake as well as good selectivity and permeability, they are made up by heavy elements in their structures. Therefore, the net of gravimetric densities reported in term of wt% are commonly quite low. Moreover, MOFs are generally known to have low structural stability at certain conditions (e.g. high temperature, acidic environment) and they are less resistant to the nucleophilic attack of water molecules [2]. Unfortunately, post-combustion flue gas commonly bear water vapour at a relatively high temperature. A class of carbon-based materials that is investigated in this work is the well-known carbon nanotubes (CNTs), in particular the single walled CNTs (SWCNTs). SWCNTs are one-dimensional carbon structures that are equipped with an intrinsic cavity inside the tubular-like structures. The large available volume within SWCNTs promises the possibility for CO_2 confinement. With their robust and light-weight structures, it is beneficial to exploit SWCNTs capacity as CO_2 capture and storage materials suitable to be

used in movable/mobile platforms. The phenomenon of adsorption dynamics and the corresponding mechanism as the effect of diameter and chirality are still an important line of research [26]. Accordingly, a preliminary study using a computational modelling and running simulations is crucial to gain atomistic perception into the interactions [27–29].

Molecular dynamics (MD) simulations performed by using accurate intramolecular and intermolecular potentials are a strength tool to describe particular dynamical adsorption system and to get practical energetic details at a given temperature [30]. Although some molecular dynamics simulations have also been implemented to study the CO_2 adsorption on CNTs [31,32], in this work the emphasis is on the accuracy of the intermolecular and intramolecular potentials. These potentials have been modelled and specifically formulated for CO_2 and CNTs by adopting an improved representation of the van der Waals contribution and by applying flexibility to CNTs structures. In comparison with this work, three charge-site of CO_2 models, rigid CNTs and the conventional Lennard-Jones potential were used in reported literatures [31,32]. This work is a continuation of a previous work of our group in which different types of SWCNTs have succesfully been exploited [33].

2 Computational Methods

The total potential energy function, V_{total}, adopted to calculate the total interaction energy for CO_2 molecules and the SWCNT is formulated as a sum of two separable terms. Of these, one, denoted as V_{SWCNT}, accounts for the SWCNT intramolecular potential energy, and the other one, denoted as $V_{intermol}$, accounts for the intermolecular potential energy of the SWCNT–CO_2 and CO_2–CO_2 interacting pairs:

$$V_{total} = V_{SWCNT} + V_{intermol} \tag{1}$$

where

$$V_{intermol} = \sum_{i=1}^{l}\sum_{j=1}^{n} V_{C_i-(CO_2)_j} + \sum_{j=1}^{n-1}\sum_{k>j}^{n} V_{(CO_2)_j-(CO_2)_k} \tag{2}$$

In the above equation n is the amount of CO_2 molecules, while l represents the number of carbon atoms in the SWCNT.

2.1 Bonding Interactions in SWCNT

In the course of MD simulations, the carbon nanostructures were allowed to vibrate to reproduce the consequent out-of-plane movements of SWCNT surfaces by adopting intramolecular potential reported in Ref [34]. The corresponding intramolecular potential (V_{SWCNT} in Eq. 1) of flexible SWCNT is computed as a sum of potential energy terms depending on bond lengths, bending angles and dihedral angles, as follows:

$$V_{SWCNT} = \sum U(r_{ij}) + \sum U(\theta_{ijk}) + \sum U(\phi_{ijkl}) \tag{3}$$

where the r_{ij}'s are the interparticle distances, the θ_{ijk}'s are the bending angles between triples of consecutive atoms i, j, k and ϕ_{ijkl} is the dihedral angle defined by a given set of four consecutive C atoms of the SWCNT; summation, running over atom indices, is intended to avoid redundant terms. The stretching potential $\mathrm{U}(r_{ij})$ of a C–C interatomic bond in the SWCNT is framed as a Morse potential function:

$$U(r_{ij}) = E_0[\{1 - \exp(-k_M(r_{ij} - r_0))\}^2 - 1] \tag{4}$$

where r_{ij} represents the interatomic radius between C atom i and j, E_0 is the well depth (114.4569 kcal mol^{-1} Å^{-2}), r_0 is the equilibrium distance (1.418 Å) and $k_M = 2.1867$ Å^{-1} is connected to the bond force constant.

Valence angle potential ($\mathrm{U}(\theta_{ijk})$) terms for the bond bending of nanotubes are formulated by harmonic cosine functions:

$$U(\theta_{jik}) = \frac{k}{2}(\cos(\theta_{jik}) - (\cos(\theta_0))^2 \tag{5}$$

θ_{jik} represents the angle between C_j-C_i-C_k atoms, θ_0 is the equilibrium value (120°), while k is the force constant (134.5 kcal mol^{-1}). A cosine function is used for the dihedral angle potentials ($\mathrm{U}(\phi_{ijkl})$), describing the interaction arising from torsional forces involving atom C_i-C_j-C_k-C_l, where the parameter values A is fixed at 6.0096 kcal kcal mol^{-1}.

$$U(\phi_{ijkl}) = \frac{1}{2}A(1 - \cos(2\phi_{ijkl})) \tag{6}$$

2.2 CO_2-SWCNT and CO_2-CO_2 Interactions

Describing correctly the intermolecular potential ($\mathrm{V}_{intermol}$) is essential in order to obtain accurate results in a MD simulation. In this study, the intermolecular forces of interest are those occurring between CO_2 molecules and between CO_2 and SWCNT. Electrostatic and non-electrostatic contributions are the two components that composed the intermolecular interaction energy. The electrostatic part can be simply determined by using the Coulomb law. On the other hand, the non-electrostatic contribution is evaluated by taking into consideration the pairwise induction and dispersion long range attractive interactions and short range repulsion, which add up resulting in the van der Waals forces, which are expressed for each interacting pairs using the so-called Improved Lennard-Jones (ILJ) pairwise function [35–37]:

$$V_{ILJ}(r) = \varepsilon \left[\frac{m}{n(r) - m} \left(\frac{r_0}{r}\right)^{n(r)} - \frac{n(r)}{n(r) - m} \left(\frac{r_0}{r}\right)^{m} \right] \tag{7}$$

In the Eq. 7, the parameters ε and r_0 correspond to the well depth and the equilibrium position of the given interacting pair, respectively. m has the value of 1 for ion-ion, 4 for ion-neutral and 6 for neutral-neutral pairs interactions.

The left term of the Eq. 7 (inside big bracket) depicts the repulsion as a function of the distance r, while the right term in the equation performs the long-range attraction. To modulate the strength of the attraction and the decline of the repulsion in Eq. 7, the $n(r)$ term is defined as follows:

$$n(r) = \beta + 4.0\left(\frac{r}{r_0}\right)^2 \tag{8}$$

where β is a parameter for modulating the hardness of the interacting pair [38]. All of the ILJ parameters that were implemented in this study were fine-tuned and benchmarked in comparison with *ab initio* calculations as reported in Ref. [39,40]. The ILJ function is much more accurate than the classical Lennard-Jones (LJ) potential function routinely used in Force-Fields for the prediction of static and dynamical properties of systems. In particular, ILJ systematically corrects the excessive long range attraction and short range repulsion of LJ potential, where the long and short-range deviations can impact adsorption dynamics. These advantages of using ILJ over conventional LJ potential have been reported in literatures [35–47].

3 Molecular Dynamics (MD) Simulations

The MD simulations were realized within the NVE microcanonical ensemble enforcing periodic boundary conditions with a rectangular cuboid box. In our MD simulations, starting from a given initial configuration, each system considered in the MD simulations was equilibrated for 0.3 ns. The production period was recorded for another 9.7 ns, leading to a total of 10 ns simulation time with a time step value set at 2.5×10^{-4} ps. The cutoff radius for the electrostatic and non-electrostatic ILJ terms were set to 19 Å to speed up the computation of the force field. The data collected during the equilibration period were excluded from the statistical analysis of the simulations for which the DL_POLY package [48] was used. Energy contributions, CO_2 distributions, gravimetric densities of CO_2 as a function of simulation time and the corresponding average values have been subsequently analyzed. The VMD software [49] has been used to construct the SWCNT structure. After the SWCNT structure were obtained, for each simulation systems, 100 CO_2 molecules were randomly added around the nanotubes surfaces at a distance of 5 to 8 Å. This corresponds to a bulk gas density value of about 89.10 g L^{-1}. A rigid type of CO_2 model reported in Ref. [39] was adopted with its point charge distributions corresponds to a five charge-site as shown in Fig. 1. This five charge-site model is more superior in treating quadrupole moment of CO_2 than the widely used three charge-site models adopted in Refs. [31,32].

We report detailed MD simulation results for 100 CO_2 molecules on the (20,0) zigzag open-ended SWCNT in comparison with our previous report of different chiralities to examine their CO_2 confinement capabilities [33]. The (20,0) SWCNT composed by five unit cells, thus it contains 400 carbon atoms (Fig. 2). The SWCNT was modelled as a non-rigid structure during MD simulations.

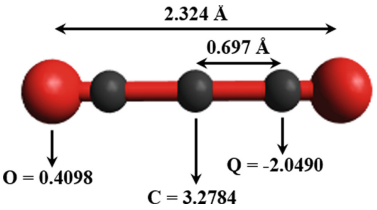

Fig. 1. Structural representation of CO_2 molecule using five charge-site model. Q is a point charge placed on the C-O bond of CO_2 molecule. The charge values are reported in a.u.

The flexibility of adsorbent materials through its molecular vibrations has been demonstrated altering its uptake capacity of adsorbing molecules such as hydrogen, nitrogen and methane [34,50]. Most importantly, treating SWCNT as a flexible structure provides more realistic representation of adsorbent and yields simulation data closer to those of the more precise results (benchmarking with respect to experimental data and higher level *ab initio* results).

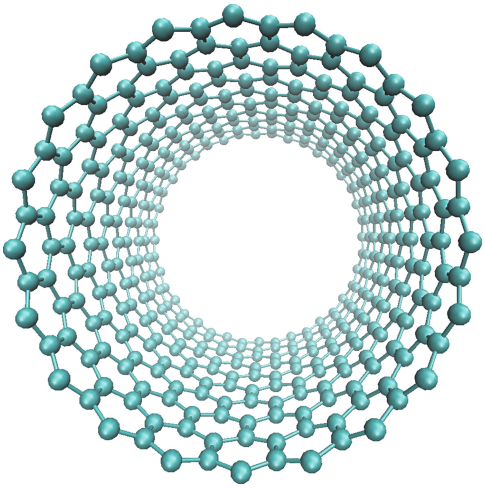

Fig. 2. (20,0) SWCNT used in the MD simulations with a diameter of 15.66 Å.

A CO_2 molecule must be within the SWCNT cavity or at a maximum distance of 7 Å from the surface of the SWCNT, in order to decide whether the CO_2 molecule is physically adsorbed. These criteria are following indications obtained in the previous works [33,40,51,52] and from the initial evaluation of radial density plots (Fig. 3). Figure 3 justifies that radius of 7 Å from CNT surface has covered the full peaks of CO_2, therefore it can be considered as adsorption region. The radial density is an analogue of z-density in which the z axis is replaced by

radius from CNT surface. It can be seen from Fig. 3 that the higher the applied temperature, the lower the radial density peak. The increase of temperature makes molecules having high kinetic energy, thus adsorption events become less effective. At 353 K, the kinetic energy at certain events can overcome repulsion forces at short-range radius. As the results, there is a small peak of CO_2 density near SWCNT surface (Fig. 3).

In order to analyze the effect of various MD parameters to the distribution of CO_2 molecules, firstly, we determined the amount of adsorbed molecules at the exohedral and endohedral sites of the carbon nanotubes. The effect of temperature on this distribution was investigated by setting three initial temperatures at 273, 300 and 353 K. Meanwhile, to investigate the dependence of the CO_2 distribution on the diameter of the SWCNT, we compare these molecular simulations with a previous work of our group involving various SWCNTs [33]. The next step was analyzing the radial distribution function to determine the composition of the repulsive and attractive interactions that exists between CO_2 molecules and the SWCNT. The summary of MD parameters and simulation results of SWCNTs are presented in Table 1.

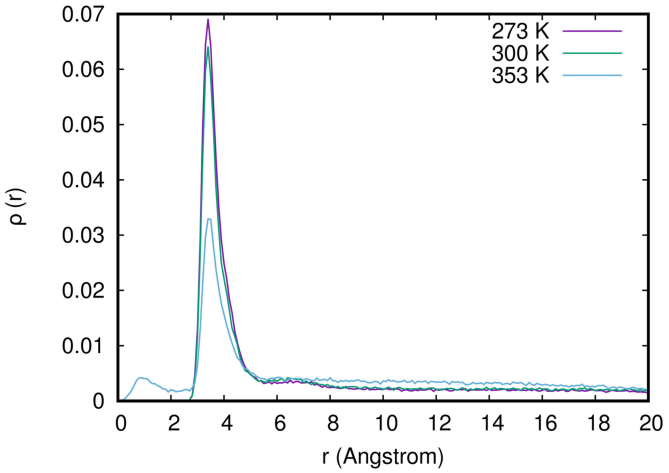

Fig. 3. Density of CO_2 inside the simulation box as function of radius from CNT surface.

Table 1 records the number of adsorbed CO_2 molecules in exohedral (N_{CO_2},out) and endohedral (N_{CO_2},in) sites simulated at NVE ensemble. The temperatures reported in Table 1 indicate the average value at the end of MD simulations. As expected, due to the adsorption phenomenon, the average temperature is lower than the initial temperature for each system. We have noticed that not all of the CO_2 molecules were physically adsorbed. Table 1 shows that the amount of CO_2 at the exohedral and endohedral sites rises with the increasing of nanotube diameter in comparison with the previous work [33]. This trend

Table 1. MD parameters and the amount of adsorbed CO_2 molecules at NVE ensemble. N_C, N_{CO_2},out and N_{CO_2}, in indicate the number of C atoms in SWCNT, the number of CO_2 molecules adsorbed outside and inside of SWCNT, respectively.

SWCNT	d (Å)	N_c	T (K)	N_{CO_2},in	N_{CO_2},out	Ref.
(5,0)	3.91	100	253.1	0 ± 0	27 ± 4	[33]
			266.8	0 ± 0	26 ± 4	
			302.8	0 ± 0	22 ± 4	
(10,0)	7.83	200	253.2	4 ± 0	43 ± 5	[33]
			277.8	4 ± 0	36 ± 7	
			305.8	4 ± 0	34 ± 4	
(15,0)	11.74	300	262.1	16 ± 1	48 ± 5	[33]
			285.6	15 ± 1	43 ± 8	
			326.8	14 ± 1	37 ± 4	
(20,0)	15.66	400	264.2	14 ± 1	53 ± 4	this work
			281.2	16 ± 1	46 ± 4	
			315.3	14 ± 1	35 ± 4	

is due to the fact that the available volume at endohedral and exohedral sites enlarges as the SWCNT diameter increases.

We also report the amount of confined CO_2 in a unit of mg g^{-1}, by considering that CO_2 molecule is confined if it is adsorbed in an endohedral site of the SWCNT. We obtained that the (20,0) structure can confine up to 146.65 mg CO_2 for 1 g of adsorbent. This value is equivalent to about 12.39 wt(%), which can fairly be considered a quite large gas uptake value. It is clear that by increasing the diameter of SWCNT, the degree of surface convexity inside the SWCNT also increases. Therefore, CO_2 confinement inside SWCNT is directly proportional with the diameter of carbon nanotubes (Table 1).

Figure 4 shows the molecular configuration after 10 ns of simulation for the (20,0) system as an illustrative example of the equilibrium. It can be seen in Fig. 4 that the endohedral site can be occupied by CO_2 to accommodate molecular confinement. In addition, the exohedral site also exhibits adsorption properties with a much higher CO_2 uptake (Table 1 and Fig. 4). Therefore, in order to provide a more quantitative ground, the total storage capacity (SC) of SWNCTs was evaluated at every step of the trajectory by calculating gravimetric density, wt(%), as the following:

$$wt\% = \frac{N_a \times M_{CO_2}}{M_{system}} \times 100 \tag{9}$$

where N_a represents the number of adsorbed CO_2, M_{CO_2} is the mass of CO_2 molecule, and M_{system} is total mass of the system including the SWCNT and the gas molecules. The adsorbed CO_2 molecules were estimated by summing CO_2 inside the cavity and those that were located at a distances of 7 Å from

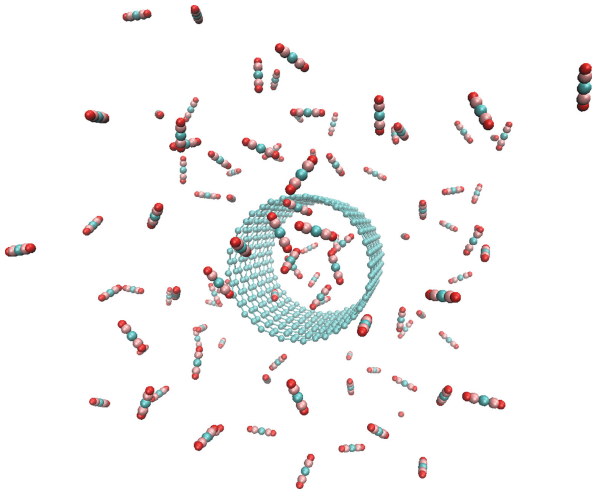

Fig. 4. Snapshot of final configuration of the (20,0) structure with 100 CO_2 molecules at 300 K.

the SWCNT surfaces [40,51,52]. SC gives us an idea regarding the amount of adsorbate that can be captured by a given amount of adsorbent at constant temperature. SC of a material is commonly expressed as a percentage by weight (wt%). At the end of each simulations, taking into account of three different temperatures; the gravimetric densities and van der Waals (vdW) energy at NVE ensemble are listed in Table 2. Note that the temperatures shown in Table 2 are the average temperatures during the MD simulations, not the initial ones.

Table 2. The vdW energy (kcal mol^{-1}) and gravimetric density (wt%) of (20,0) SWCNT at NVE ensemble.

SWCNT	d (Å)	T (K)	E_{vdW}	wt%
(20,0)	15.66	264.2	-263.05 ± 11.31	32.06 ± 4.57
		281.2	-289.19 ± 11.22	29.87 ± 2.29
		315.3	-150.64 ± 15.11	23.68 ± 4.57

We observe that the CO_2 storage capacity is inversely proportional with the temperature, the CO_2 molecules are increasingly desorbed as the temperature increases. We can try to get an idea that at high temperature the share of vdW energy, mainly responsible for adsorption, decreases (see Table 2) as well as the total potential energy. Since the total energy of system should be conserved at NVE ensemble, the decrease in the potential energy give rise to kinetic energy of the system. These factors leads to the weakening of the interaction between SWCNT and CO_2 molecules.

The manifestation of kinetic energy as well as contribution of attraction forces, leading to adsoprtion, also can be seen from Table 3 where diffusion coefficients of CO_2 molecules inside the simulation box are reported. If we compare with the previous work, in general, the maximum CO_2 storage is obtained for the SWCNT (15,0) even if it does not have the largest diameter. It seems that when the diameter increases, up to a certain limit, a competing van der Waals (vdW) attraction-repulsion contribution favour higher desorption. Nevertheless, with a relatively high CO_2 uptake, it is an early sign that this material is a good candidate for CO_2 capture and storage applications.

Table 3. The diffusion coefficients (10^{-7} m^2 s^{-1}) of four SWCNTs at NVE ensemble.

SWCNT	T (K)	D_{NVE}	Ref.
(5,0)	273	1.74	[33]
	300	1.71	
	353	1.52	
(10,0)	273	1.38	[33]
	300	1.76	
	353	2.12	
(15,0)	273	1.12	[33]
	300	1.38	
	353	2.12	
(20,0)	273	1.28	This work
	300	1.63	
	353	1.78	

The total gravimetric uptake comparison between some nanoporous materials is reported in Table 4. It shows that the (20,0) structure adsorbs CO_2 molecules up to 32.1 wt% at microcanonical NVE ensemble with an initial temperature of 273 K. This value is comparable and competitive with other materials investigated by using experimental and/or theoretical methods reported in Table 4. It can also be seen that the gravimetric values estimated from MD simulations performed using our potentials are in the same order of magnitude with the experimental results. However, all of the SWCNT gravimetric values obtained in this work are still lower than those of 3-dimensional porous carbons reported in Refs. [21] and [22], 54.3 wt% (300 K & 30 bar) and 48.1 wt% (298 K & 20 bar), respectively. This was expected to be due to the more available pores acting as adsorption sites in the 3-dimensional structure with respect to the 1-dimensional ones.

Table 4. Total gravimetric uptake comparison between various nanoporous materials.

Materials	T (K)	P (bar)	CO_2 uptake (wt%)	References
SWCNT (9,9)	298	30–60	21–23	[26]
MOFs	298	1	19.7	[53]
Graphene oxide (nanocomposite)	300	20	12.7	[54]
SWCNT	298	1.1	2.9	[55]
Nanoporous carbon	298	26	17.7	[56]
Nanosilicate	298	55	22	[57]
CNT (nanocomposite)	298	32.5	28.4	[58]
SWCNT (10,0)	253	21.7	30.6	[33]
SWCNT (10,0)	278	29.0	26.0	[33]
SWCNT (15,0)	262	17.1	34.8	[33]
SWCNT (15,0)	286	20.8	31.8	[33]
SWCNT (20,0)	264	14.9	32.1	This work
SWCNT (20,0)	281	31.6	29.9	This work

4 Conclusions

Having relatively high gas uptake and remarkable physicochemical properties of carbon-based materials, SWCNTs are equipped with a property that makes them potentially versatile materials competitive with other porous adsorbents to cope with CO_2 gas emission. Indeed, with an increase in diameter, other gas molecules can also be adsorbed by SWCNTs thus lowers the storage capacity of CO_2. However, if a material exhibits high CO_2 uptake, it is an early sign that this material is a good candidate for CO_2 capture and separation applications. Therefore, our future objective is to extensively investigate the application of SWCNTs in separating CO_2 molecules from CO_2/N_2 and CO_2/CH_4 gaseous mixtures saturated with H_2O component.

Acknowledgement. The authors thank MUR and University of Perugia for their support through the AMIS project "Dipartimenti di Eccellenza 2018–2022". NFL, AL and LP thank the Department of Chemistry, Biology and Biotechnology, University of Perugia for funding under the program "Fondo Ricerca di Base 2021" (RICBASE2021FAGINAS). NFL and AL also acknowledge support for allocation of computing time from the Oklahoma University Supercomputing Center for Education & Research (OSCER). N.F-L and A. L acknowledge also Fondazione Cassa di Risparmio di Perugia n. 220.0513 to C.E. This work is supported by a grant from Fondazione Cassa di Risparmio di Perugia n.# 220.0513 to C.E.

References

1. EPA-United States Environmental Protection Agency: Climate Change Indicators in the United States: Global Greenhouse Gas Emissions (2016)
2. Smit, B.: Carbon capture and storage: introductory lecture. Faraday Discuss. **192**, 9–25 (2016)
3. World Resources Institute: Climate Analysis Indicators Tool (CAIT) 2.0: WRI's Climate Data Explorer
4. Bui, M., et al.: Carbon capture and storage (CCS): the way forward. Energy Environ. Sci. **11**, 1062–1176 (2018)
5. Joos, L., Huck, J.M., Van Speybroeck, V., Smit, B.: Cutting the cost of carbon capture: a case for carbon capture and utilization. Faraday Discuss. **192**, 391–414 (2016)
6. Dai, N., Mitch, W.A.: Effects of flue gas compositions on nitrosamine and nitramine formation in postcombustion CO_2 capture systems. Environ. Sci. Technol. **48**(13), 7519–7526 (2014)
7. Huck, J.M., et al.: Evaluating different classes of porous materials for carbon capture. Energy Environ. Sci. **7**, 4132–4146 (2014)
8. Zhang, S., Shen, Y., Shao, P., Chen, J., Wang, L.: Kinetics, thermodynamics, and mechanism of a novel biphasic solvent for CO_2 capture from flue gas. Environ. Sci. Technol. **52**(6), 3660–3668 (2018)
9. Liu, H., et al.: A hybrid absorption-adsorption method to efficiently capture carbon. Nat. Commun. **5**, 5147 (2014)
10. Lu, A.H., Hao, G.P.: Porous materials for carbon dioxide capture. Annu. Rep. Prog. Chem. Sect. A: Inorg. Chem. **109**, 484–503 (2013)
11. Li, J.R., et al.: Porous materials with pre-designed single-molecule traps for CO_2 selective adsorption. Nat. Commun. **4**, 1538 (2014)
12. Hu, X.E., et al.: A review of n-functionalized solid adsorbents for post-combustion CO_2 capture. Appl. Energy **260**, 114244 (2020)
13. Du, H., Li, J., Zhang, J., Su, G., Li, X., Zhao, Y.: Separation of hydrogen and nitrogen gases with porous graphene membrane. J. Phys. Chem. C **115**(47), 23261–23266 (2011)
14. Kim, J., Lin, L.C., Swisher, J.A., Haranczyk, M., Smit, B.: Predicting large CO_2 adsorption in aluminosilicate zeolites for postcombustion carbon dioxide capture. J. Am. Chem. Soc. **134**(46), 18940–18943 (2012)
15. Liu, B., Smit, B.: Molecular simulation studies of separation of CO_2/N_2, CO_2/CH_4, and CH_4/N_2 by ZIFs. J. Phys. Chem. C **114**(18), 8515–8522 (2010)
16. Schrier, J.: Carbon dioxide separation with a two-dimensional polymer membrane. ACS Appl. Mater. Interfaces **4**(7), 3745–3752 (2012)
17. Zeng, Y., Zou, R., Zhao, Y.: Covalent organic frameworks for CO_2 capture. Adv. Mater. **28**(15), 2855–2873 (2016)
18. Xiang, Z., et al.: Systematic tuning and multifunctionalization of covalent organic polymers for enhanced carbon capture. J. Am. Chem. Soc. **137**(41), 13301–13307 (2015)
19. Yu, J., Xie, L.H., Li, J.R., Ma, Y., Seminario, J.M., Balbuena, P.B.: CO_2 capture and separations using MOFs: computational and experimental studies. Chem. Rev. **117**(14), 9674–9754 (2017)
20. Lin, L.C., et al.: Understanding CO_2 dynamics in metal-organic frameworks with open metal sites. Angew. Chem. Int. Ed. **52**(16), 4410–4413 (2013)

21. Srinivas, G., Krungleviciute, V., Guo, Z.X., Yildirim, T.: Exceptional CO_2 capture in a hierarchically porous carbon with simultaneous high surface area and pore volume. Energy Environ. Sci. **7**, 335–342 (2014)
22. Ganesan, A., Shaijumon, M.: Activated graphene-derived porous carbon with exceptional gas adsorption properties. Microporous Mesoporous Mater. **220**, 21–27 (2015)
23. Ghosh, S., Sevilla, M., Fuertes, A.B., Andreoli, E., Ho, J., Barron, A.R.: Defining a performance map of porous carbon sorbents for high-pressure carbon dioxide uptake and carbon dioxide-methane selectivity. J. Mater. Chem. A **4**, 14739–14751 (2016)
24. Bartolomei, M., Carmona-Novillo, E., Giorgi, G.: First principles investigation of hydrogen physical adsorption on graphynes' layers. Carbon **95**, 1076–1081 (2015)
25. Apriliyanto, Y.B., Battaglia, S., Evangelisti, S., Faginas-Lago, N., Leininger, T., Lombardi, A.: Toward a generalized hückel rule: the electronic structure of carbon nanocones. J. Phys. Chem. A **125**(45), 9819–9825 (2021)
26. Lithoxoos, G.P., Labropoulos, A., Peristeras, L.D., Kanellopoulos, N., Samios, J., Economou, I.G.: Adsorption of N_2, CH_4, CO and CO_2 gases in single walled carbon nanotubes: A combined experimental and monte carlo molecular simulation study. J. Supercrit. Fluids **55**(2), 510–523 (2010)
27. Lombardi, A., Lago, N.F., Laganà, A., Pirani, F., Falcinelli, S.: A bond-bond portable approach to intermolecular interactions: simulations for N-methylacetamide and carbon dioxide dimers. In: Murgante, B. (ed.) ICCSA 2012. LNCS, vol. 7333, pp. 387–400. Springer, Heidelberg (2012). https://doi.org/10.1007/978-3-642-31125-3_30
28. Lombardi, A., Faginas-Lago, N., Pacifici, L., Costantini, A.: Modeling of energy transfer from vibrationally excited CO_2 molecules: Cross sections and probabilities for kinetic modeling of atmospheres, flows, and plasmas. J. Phys. Chem. A **117**(45), 11430–11440 (2013)
29. Falcinelli, S., Rosi, M., Candori, P., Vecchiocattivi, F., Bartocci, A., Lombardi, A., Lago, N.F., Pirani, F.: Modeling the intermolecular interactions and characterization of the dynamics of collisional autoionization processes. In: Murgante, B. (ed.) ICCSA 2013. LNCS, vol. 7971, pp. 69–83. Springer, Heidelberg (2013). https://doi.org/10.1007/978-3-642-39637-3_6
30. DuBay, K.H., Hall, M.L., Hughes, T.F., Wu, C., Reichman, D.R., Friesner, R.A.: Accurate force field development for modeling conjugated polymers. J. Chem. Theory Comput. **8**(11), 4556–4569 (2012)
31. Rahimi, M., Singh, J.K., Babu, D.J., Schneider, J.J., Müller-Plathe, F.: Understanding carbon dioxide adsorption in carbon nanotube arrays: molecular simulation and adsorption measurements. J. Phys. Chem. C **117**(26), 13492–13501 (2013)
32. Alexiadis, A., Kassinos, S.: Molecular dynamic simulations of carbon nanotubes in CO_2 atmosphere. Chem. Phys. Lett. **460**(4–6), 512–516 (2008)
33. Faginas-Lago, N., Apriliyanto, Y.B., Lombardi, A.: Confinement of CO_2 inside carbon nanotubes. Eur. Phys. J. D **75**(5), 1–10 (2021). https://doi.org/10.1140/epjd/s10053-021-00176-7
34. Faginas-Lago, N., Yeni, D., Huarte, F., Wang, Y., Alcamí, M., Martin, F.: Adsorption of hydrogen molecules on carbon nanotubes using quantum chemistry and molecular dynamics. J. Phys. Chem. A **120**(32), 6451–6458 (2016)
35. Pirani, P., Brizi, S., Roncaratti, L., Casavecchia, P., Cappelletti, D., Vecchiocattivi, F.: Beyond the lennard-jones model: a simple and accurate potential function probed by high resolution scattering data useful for molecular dynamics simulations. Phys. Chem. Chem. Phys. **10**, 5489 (2008)

36. Lombardi, A., Laganà, A., Pirani, F., Palazzetti, F., Lago, N.F.: Carbon oxides in gas flows and earth and planetary atmospheres: state-to-state simulations of energy transfer and dissociation reactions. In: Murgante, B. (ed.) ICCSA 2013. LNCS, vol. 7972, pp. 17–31. Springer, Heidelberg (2013). https://doi.org/10.1007/978-3-642-39643-4_2
37. Albertí, M., Lago, N.F.: Ion size influence on the Ar solvation shells of $M^+C_6F_6$ clusters (M = Na, K, Rb, Cs). J. Phys. Chem. A **116**(12), 3094–3102 (2012)
38. Pirani, F., Albertí, M., Castro, A., Moix Teixidor, M., Cappelletti, D.: Atom-bond pairwise additive representation for intermolecular potential energy surfaces. Chem. Phys. Lett. **394**(1–3), 37–44 (2004)
39. Lombardi, A., Pirani, F., Laganà, A., Bartolomei, M.: Energy transfer dynamics and kinetics of elementary processes (promoted) by gas-phase CO_2-N_2 collisions: Selectivity control by the anisotropy of the interaction. J. Comput. Chem. **37**(16), 1463–1475 (2016)
40. Apriliyanto, Y.B., Faginas Lago, N., Lombardi, A., Evangelisti, S., Bartolomei, M., Leininger, T., Pirani, F.: Nanostructure selectivity for molecular adsorption and separation: the case of graphyne layers. J. Phys. Chem. C **122**(28), 16195–16208 (2018)
41. Pacifici, L., Verdicchio, M., Lago, N.F., Lombardi, A., Costantini, A.: A high-level ab initio study of the N_2 + N_2 reaction channel. J. Comput. Chem. **34**(31), 2668–2676 (2013)
42. Faginas Lago, N., Huarte Larrañaga, F., Albertí, M.: On the suitability of the ILJ function to match different formulations of the electrostatic potential for water-water interactions. Eur. Phys. J. D **55**(1), 75–85 (2009). https://doi.org/10.1140/epjd/e2009-00215-5
43. Albertí, M., Lago, N.F.: Competitive solvation of K^+ by C_6H_6 and H_2O in the K^+-$(C_6H_6)_n$-$(H_2O)_m$ (n=1-4; m=1-6) aggregates. Eur. Phys. J. D **67**(4), 73 (2013). https://doi.org/10.1140/epjd/e2013-30753-x
44. Faginas-Lago, N., Lombardi, A., Albertí, M., Grossi, G.: Accurate analytic intermolecular potential for the simulation of Na^+ and K^+ ion hydration in liquid water. J. Mol. Liq. **204**, 192–197 (2015)
45. Faginas Lago, N., Albertí, M., Lombardi, A., Pirani, F.: A force field for acetone: the transition from small clusters to liquid phase investigated by molecular dynamics simulations. Theor. Chem. Acc. **135**(7), 1–9 (2016). https://doi.org/10.1007/s00214-016-1914-9
46. Lombardi, A., Faginas-Lago, N., Gaia, G., Federico, P., Aquilanti, V.: Collisional energy exchange in CO_2–N_2 gaseous mixtures. In: Gervasi, O., Murgante, B., Misra, S., Rocha, A.M.A.C., Torre, C., Taniar, D., Apduhan, B.O., Stankova, E., Wang, S. (eds.) ICCSA 2016. LNCS, vol. 9786, pp. 246–257. Springer, Cham (2016). https://doi.org/10.1007/978-3-319-42085-1_19
47. Faginas-Lago, N., Apriliyanto, Y.B., Lombardi, A.: Carbon capture and separation from $CO_2/N_2/H_2O$ gaseous mixtures in bilayer graphtriyne: a molecular dynamics study. In: Gervasi, O. (ed.) ICCSA 2020. LNCS, vol. 12255, pp. 489–501. Springer, Cham (2020). https://doi.org/10.1007/978-3-030-58820-5_36
48. Smith, W., Yong, C., Rodger, P.: `DL_POLY`: application to molecular simulation. Mol. Simul. **28**(5), 385–471 (2002)
49. Humphrey, W., Dalke, A., Schulten, K.: VMD: visual molecular dynamics. J. Mol. Graph. **14**(1), 33–8 (1996)
50. Vekeman, J., Sánchez-Marín, J., de Sánchez Merás, A., Garcia Cuesta, I., Faginas-Lago, N.: Flexibility in the graphene sheet: the influence on gas adsorption from molecular dynamics studies. J. Phys. Chem. C **123**(46), 28035–28047 (2019)

51. Faginas-Lago, N., Apriliyanto, Y.B., Lombardi, A.: Molecular simulations of $CO_2/N_2/H_2O$ gaseous mixture separation in graphtriyne membrane. In: Misra, S. (ed.) ICCSA 2019. LNCS, vol. 11624, pp. 374–387. Springer, Cham (2019). https://doi.org/10.1007/978-3-030-24311-1_27
52. Apriliyanto, Y.B., Darmawan, N., Faginas-Lago, N., Lombardi, A.: Two-dimensional diamine-linked covalent organic frameworks for CO_2/N_2 capture and separation: theoretical modeling and simulations. Phys. Chem. Chem. Phys. **22**, 25918–25929 (2020)
53. Spanopoulos, I., et al.: Exceptional gravimetric and volumetric CO_2 uptake in a palladated NbO-type MOF utilizing cooperative acidic and basic, metal-CO_2 interactions. Chem. Commun. **52**(69), 10559–10562 (2016)
54. Rodríguez-García, S., et al.: Role of the structure of graphene oxide sheets on the CO_2 adsorption properties of nanocomposites based on graphene oxide and polyaniline or Fe_3O_4-nanoparticles. ACS Sustain. Chem. Eng. **7**(14), 12464–12473 (2019)
55. Osler, K., Dheda, D., Ngoy, J., Wagner, N., Daramola, M.O.: Synthesis and evaluation of carbon nanotubes composite adsorbent for CO_2 capture: a comparative study of CO_2 adsorption capacity of single-walled and multi-walled carbon nanotubes. Int. J. Coal Sci. Technol. **4**(1), 41–49 (2017). https://doi.org/10.1007/s40789-017-0157-2
56. Patzsch, J., Babu, D.J., Schneider, J.J.: Hierarchically structured nanoporous carbon tubes for high pressure carbon dioxide adsorption. Beilstein J. Nanotechnol. **8**(1), 1135–1144 (2017)
57. Cavalcanti, L.P., Kalantzopoulos, G.N., Eckert, J., Knudsen, K.D., Fossum, J.O.: A nano-silicate material with exceptional capacity for CO_2 capture and storage at room temperature. Sci. Rep. **8**(1), 1–6 (2018)
58. Puthusseri, D., Babu, D.J., Okeil, S., Schneider, J.J.: Gas adsorption capacity in an all carbon nanomaterial composed of carbon nanohorns and vertically aligned carbon nanotubes. Phys. Chem. Chem. Phys. **19**(38), 26265–26271 (2017)